Available online at www.sciencedirect.com
ScienceDirect
Nuclear Physics B Proceedings Supplement 00 (2014) 1–7
Nuclear Physics B Proceedings Supplement

Design options for the upgrade of the CMS electromagnetic calorimeter

R. Paramatti on behalf of the CMS Collaboration

INFN - Roma
email: riccardo.paramatti@roma1.infn.it

Abstract

The CMS scintillating lead-tungstate calorimeter was designed to operate for at least ten years at the LHC, assuming an instantaneous luminosity of 10^{34} cm^{-2} s^{-1}. The measurements obtained with data collected in LHC Run1 (2010-2012) show that the detector has performed according to design specifications and will survive with excellent performance through the lifetime of the LHC. However, plans for an upgrade of the LHC (the High Luminosity LHC, HL-LHC, project) aim at accumulating a much higher integrated luminosity, up to 3000 fb^{-1} in ten years. This will expose the detector to a total irradiation about six times higher with respect to the design specifications.

An intense campaign of activities has started to define the improvements needed to survive such an increase in irradiation levels. The activities carried out include irradiation studies, simulations, design, realisation and test of prototypes of new detectors that may substitute the present one in the endcap regions.

The options currently under study and the results obtained so far on the subjects outlined above will be presented.

Keywords: electromagnetic calorimeter, scintillation, crystal, lead-tungstate, radiation, upgrade, HL-LHC

1. Introduction

The CMS calorimeters were designed to operate over ten years of data-taking at LHC corresponding to a total luminosity of 500 fb^{-1} and at a maximum instantaneous luminosity of $1 \cdot 10^{34}$cm^{-2}s^{-1}. The planned High-Luminosity (HL)-LHC phase will require a significant extension of the calorimeter longevity to run for about 25 years in a much more severe radiation environment, collecting a luminosity of 3000 fb^{-1} at a peak instantaneous luminosity five times higher. Moreover the calorimeters should provide, during the HL-LHC phase, performance similar to the ones delivered during LHC Run1 phase in terms of electron and photon reconstruction efficiency, energy resolution and identification for the electromagnetic part and measurements of jets and missing transverse energy for the hadronic part.

In this report the expected performance of the current CMS electromagnetic calorimeter at HL-LHC is shown, with the focus on the degradation of energy resolution in the high pseudo-rapidity region, and the proposed replacement of the endcap part is motivated and described.

2. The electromagnetic calorimeter of CMS

The CMS ECAL is a compact and homogeneous calorimeter made of 75848 lead-tungstate ($PbWO_4$) crystals, arranged in a quasi-projective geometry [1]. The barrel region (EB) covers a pseudorapidity range up to $|\eta| = 1.48$ while the two endcaps (EE) extend up to $|\eta| < 3.0$. The scintillation light is readout with avalanche photodiodes (APDs) in EB and with vacuum phototriodes (VPTs) in EE. The transverse size of the crystals is very close to the $PbWO_4$ Molière radius of 2.2 cm while the crystal depth is about 26 and 25 radiation lengths ($X_0 = 0.89$ cm) respectively in EB and EE. A preshower detector (ES), based on lead absorbers equipped with silicon strip sensors, is placed in front of the endcap crystals.

3. Performance of CMS ECAL during HL-LHC

The HL-LHC conditions are a significant challenge to both detector longevity and performance. The challenge is particularly difficult in the endcap region, where the radiation levels have a strong gradient along η and typically change by a factor 100 between $|\eta| = 1.48$ and $|\eta| = 3.0$.

For the full 3000 fb^{-1} planned for HL-LHC, the high-energy charged hadron fluence at $|\eta|$ =2.6 in the ECAL will be $2{\cdot}10^{14}$ particle/cm^2 and the absorbed dose will be 300 kGy with an expected dose rate of 30 Gy/h. As discussed below, these dose and fluence levels would result in significant loss to the crystal light transmission and the photo-detector (VPT) performance and motivate the replacement of the endcap calorimeter of CMS for HL-LHC.

In the barrel ECAL, radiation damage is not problematic even at the highest η. However, the EB detector has to cope with higher pile-up and increased photodetector (APD) noise resulting from the foreseen instantaneous luminosity of $5{\cdot}10^{34}$cm^{-2}s^{-1}. For these reasons, keeping a high trigger efficiency is a challenge. Finally the electronics must be upgraded to meet the Level 1 readout rate and latency requirements (see Section 4).

Lead tungstate crystals are subject to two types of damage: electromagnetic and hadron irradiation damage. The effects of ionizing electromagnetic radiation on lead tungstate were studied in depth using γ radiation from ^{60}Co sources. The crystal light transmission is reduced through the formation of colour centres, while the scintillation mechanism is unchanged. The crystal transparency largely recovers through spontaneous annealing at room temperature [2]. The light output tends towards an equilibrium level, which depends on the dose rate. A precise monitoring system using injected laser light at 447 nm is used to track and correct for response changes during LHC operation.

The dominant concern for HL-LHC is the loss of response due to hadron irradiation. In CMS the flux of fast hadrons is dominated by charged pions with energies of order 1 GeV. The effect of charged hadrons has been studied on crystals irradiated with pions and protons from the CERN Proton Synchrotron [3, 4]. Figure 1 shows that the band edge of the transmission spectrum is shifted to higher wavelengths, the transmission is attenuated and therefore the light output is seriously affected. Contrary to the electromagnetic radiation, this damage is cumulative and does not anneal out at room temperature.

An extensive test-beam campaign on hadron irradiated matrices of 3×3 crystals has been performed to measure the degradation of the energy resolution for several hadron fluences [5]. The results are shown in Figure 2 where the irradiation dose is expressed in terms of the radiation induced absorption coefficient $\mu_{\rm ind}(\lambda)$:

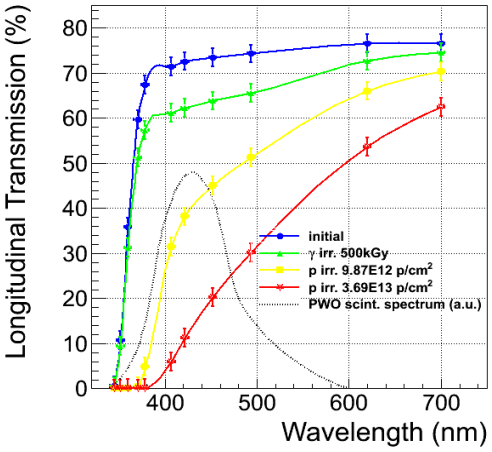

Figure 1: Light transmission of lead tungstate crystals as a function of the wavelength after proton and Co60 photon irradiation; the scintillation spectrum of the crystal is superimposed.

$$\mu_{\rm ind}(\lambda) = -\frac{1}{L} \cdot ln\left(\frac{LTO(\lambda)}{LTO_0(\lambda)}\right) \quad (1)$$

where LTO is the attenuation of the optical transmission along the crystal length L, with respect to its initial value LTO_0. The $\mu_{\rm ind}(\lambda)$ is found to be linearly dependent on the hadron fluence in the range of fluence under study ($5 \cdot 10^{11}$ to $5 \cdot 10^{13}$protons/cm^2) [3, 4].

The worsening of the energy resolution with the increasing dose, from a non-irradiated crystal matrix (μ_{ind} = 0 m^{-1}) up to the equivalent dose at the end of HL-LHC in the region $|\eta|$ = 2.6 (μ_{ind} = 20 m^{-1}), is clearly visible in the figure. The beam test has also shown that the linearity and timing response of the calorimeter are also degraded at high values of $\mu_{\rm ind}$.

Based on the above measurements, a model of crystal ageing has been developed. The radiation damage is modelled using the MARS simulation [6] for the hadron fluence and γ dose estimate and the experimental results for the attenuation of the optical transmission. A full simulation of the electromagnetic shower development in the crystals is performed with Geant4 [7]. The ray-tracing program SLitrani [8] is used to model the light output as a function of $\mu_{\rm ind}$. The γ damage is simulated as a function of the instantaneous luminosity, by assuming the equilibrium value of the light transmission is reached. The hadron damage is simulated by modelling the value of $\mu_{\rm ind}$ measured in [3] as a function of

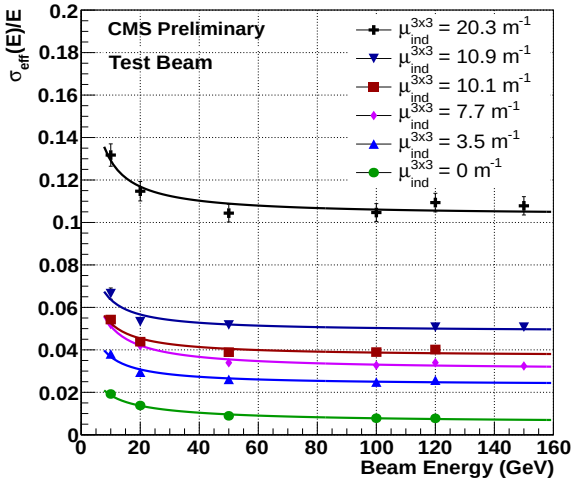

Figure 2: Energy resolution measured with electron beam on hadron irradiated crystals with different dose from non irradiated crystal (μ_{ind} = 0 m^{-1}) up to the equivalent dose at the end of HL-LHC in the region $|\eta|$ = 2.6 (μ_{ind} = 20 m^{-1})

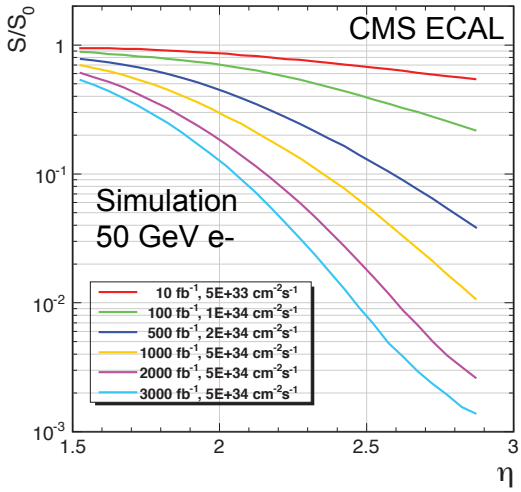

Figure 3: Relative light output S/S_0 for an electron shower of 50 GeV as a function of crystal pseudorapidity, estimated with the model described in the text, for different ageing conditions.

the hadron fluence.

Figure 3 shows the predicted response reduction, S/S_0, for an electron shower of 50 GeV as a function of η for various integrated luminosities. The uncertainty in this prediction is about 30%, and it comes from uncertainty in the hadron fluence and γ dose estimates, spread in the crystal response to γ radiation, uncertainty in the effects of the hadron radiation on the crystals, and extrapolation of these effects from low to high fluence. Based on the aging model, the barrel ($|\eta| < 1.48$) will suffer less than a factor of 2 light output loss up to 3000 fb^{-1}, while in the endcaps there will be a factor of more than 10 reduction after 3000 fb^{-1} for $\eta > 2$. The large response reduction causes an unacceptable worsening of the energy resolution of electrons and photons, requiring the replacement of the endcap part of the calorimeter.

More in detail, the reduction of scintillation light output with respect to undamaged crystals affects the energy resolution causing:

- a degradation of the stochastic term due to the reduced light output, proportional to $\sqrt{S_0/S}$
- an amplification of the noise term due to the increasing energy equivalent noise, proportional to S_0/S,
- a worsening of the constant term due to the increased light collection non-uniformity along the crystal depth z, proportional to $\partial(S/S_0)/\partial z$.

3.1. Ageing of Avalanche Photodiodes

The ECAL barrel APDs are silicon photodiodes with internal gain, developed and produced by Hamamatsu Photonics in collaboration with CMS. They are operated at gain $G = 50$ and at a temperature of 18^{o}C. As with all silicon devices, they are sensitive to γ and hadron damage [9]. The γ radiation causes an increase in the surface current and decreases the quantum efficiency. However the principal concern for the HL-LHC is hadron damage. Neutrons dominate the hadron spectrum behind the ECAL crystals. Hadrons create defects in the silicon bulk which induce an increase in dark current of the detector and consequently in the levels of electronic noise. The evolution of the dark current of APDs in channels located at different pseudorapidity during LHC Run1 is shown in Figure 4 together with the LHC delivered luminosity as a function of time. These data confirm the linearity in the rate of creation of defects in the APD with neutron fluence. During technical stops and winter shutdowns a part of the APD defects anneals and the current reduces.

The neutron fluence predicted with the FLUKA simulation [10] is about $\Phi_n = 1.2 - 2.4 \cdot 10^{14}$ n/cm^2 (1 MeV neutron equivalent) at $\eta = 0 - 1.45$ for a delivered luminosity of 3000 fb^{-1}. The expected dark current of a pair of APDs at gain 50 at $\eta = 1.45$, considering only the permanent bulk damage, is 200-250 μA. Other effects due to neutron damage at high fluences are a shift of the bias voltage required to obtain a gain of 50 and a

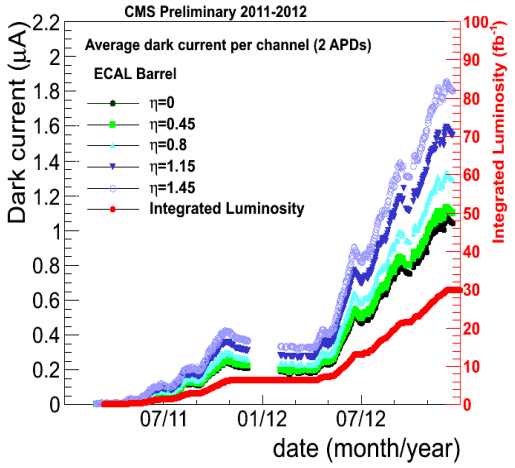

Figure 4: Evolution of the dark current in Avalanche Photodiodes installed in the ECAL Barrel for different pseudorapidity during LHC Run1. The red points show the LHC delivered luminosity as a function of time. During technical stops and winter shutdowns a partial reduction of the current is observed.

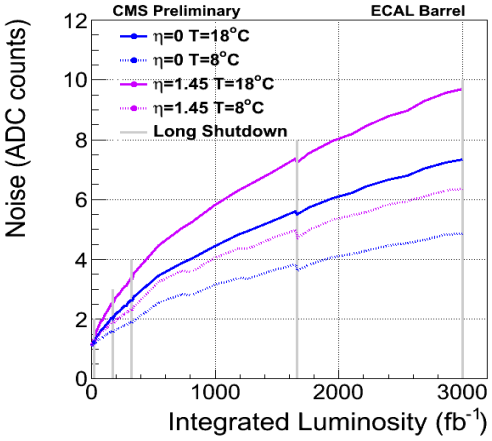

Figure 5: Expected noise with current ECAL electronics as a function of LHC integrated luminosity in the centre of the Barrel ($|\eta| = 0$) and at the edge ($|\eta| = 1.45$). The expected noise is shown also in the case of the decreasing of the ECAL operating temperature to 8 °C.

reduction of quantum efficiency.

The preamplifier noise depends on the square root of the APD bulk current times the shaping time τ, which is currently 43 ns. The evolution of noise as a function of the dark current has been measured with APDs irradiated up to the HL-LHC expected fluence. The noise is expected to increase up to 9-10 ADC counts for a dark current of 200-250 μA (one ADC count corresponds to about 40 MeV). Figure 5 shows the predicted increase of the noise as a function of the integrated luminosity with the present ECAL electronics. The noise levels in EB will reach almost 350 MeV per channel at $\eta = 1.45$ after 3000 fb^{-1}, neglecting changes in crystal light output and quantum efficiency. Considering that electromagnetic showers in ECAL are typically reconstructed summing the energy of at least a 5×5 crystal matrix, the level of electronics noise will be the limiting factor of the EB energy resolution for photons after 1500 fb^{-1}.

The APD dark current is strongly dependent on the temperature and a reduction of a factor 2.5 in dark current is expected if the ECAL operating temperature is reduced from 18 to 8 °C, which translates into a reduction of the noise by 35%. Figure 5 also presents the expected noise levels in the detector at lower temperature and it shows that operating the APDs at 8°C after 3000 fb^{-1} corresponds in terms of noise to operating at 18°C after about 1000-1200 fb^{-1}.

4. New Barrel Electronics

In the present calorimeter, the channel readout is formed by two APDs mounted on the rear face of the crystal and connected in parallel. The APDs are connected to the passive motherboard (MB) which distributes high voltage and low voltage and connects the APDs to the very-front-end (VFE) cards. Each VFE card has five readout channels consisting of a multi-gain pre-amplifier (MPGA) with a 43 ns shaping time and a 12-bit analog-to-digital converter (ADC). The digitized signals from five VFE cards are passed to an FE card. The FE card forms the trigger primitive for the 5×5 crystal array and contains a digital latency buffer and the primary event buffer. All the boards were tested to resist the radiation environment of the ECAL endcaps and for ten-year operation.

The trigger primitive consists of the transverse energy deposited in a trigger tower (the 5×5 crystal array) and a single bit to qualify the energy deposit along η. The per-crystal information is buffered in the FE for transmission to the data concentrator card, with a maximum latency in the event buffer of 6.4 μs and a maximum Level 1 accept rate of about 100 kHz.

The ECAL barrel electronics will be replaced to meet the requirements of the Phase 2 Level 1 trigger system, which foresees an increase of the latency up to 20 μs and an increase of the bandwidth up to 1 MHz. This upgrade will also allow the provision of individual crystal information to the Level 1 calorimeter trigger. By including the VFE in the upgrade, the pulse shaping and sampling can be optimised to mitigate the increase in APD noise

and pile-up and improve timing resolution. Finally it will reduce the risk of using electronics for 30 years and 3000 fb^{-1} that were designed for 10 years running and 500 fb^{-1}.

The performance goals of the EB upgrade can be achieved through the replacement of the VFE and FE cards, together with the associated low-voltage distribution system and optical links, without changing the APDs and the motherboards as there is no identified concern with these items. Figure 6 shows a possible new architecture. The individual boards will follow the same configuration and form factor as the present electronics in order to fit into the same physical space and use the existing services whenever possible.

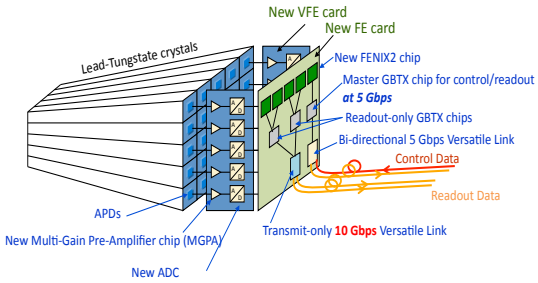

Figure 6: A possible new architecture for the upgraded ECAL Barrel Electronics.

5. The Endcap Calorimetry Upgrade

As discussed above, the physics performance of CMS ECAL in the HL-LHC phase will be significantly compromised without the replacement of the endcap part.

Two conceptual designs for the replacement of endcap calorimetry systems are presented here. One design proposes a standalone tungsten/LYSO(CeF_3) sampling electromagnetic calorimeter optimised for a small Moliere radius and high radiation tolerance, followed by a full-depth hadron calorimeter based on scintillators. In the second conceptual design the endcaps of both the electromagnetic and hadronic calorimeters are replaced by a silicon-based calorimeter with a very high transverse and longitudinal granularity to manage pile-up by tracking shower development in detail.

5.1. New sampling ECAL Endcap

The EE sampling structure proposed here uses a very dense design to minimize the effects of pile-up. The structure consists of alternating layers of dense absorber and scintillating crystal tiles. Various materials have been simulated using standalone GEANT4 and fast simulation techniques and the sampling combination of tungsten absorbers with LYSO(Ce) or CeF_3 scintillators provides the best energy resolution, dimensional compactness, and the highest light yield for electromagnetic calorimetry in the endcap/forward region, comparable with the light yield of NaI. These combinations can provide an energy resolution of about $10\%/\sqrt{E}$ and excellent potential for minimizing the effects of pile-up due to the small Molière radius (14 mm for the W/LYSO combination to be compared with 21 mm of the lead tungstate) with a very similar emission wavelength and decay time. The new calorimeter will also be more compact with respect to the current ECAL endcap thanks to the shorter radiation length: 5.1 mm and 8.9 mm respectively for the W/LYSO and the $PbWO_4$.

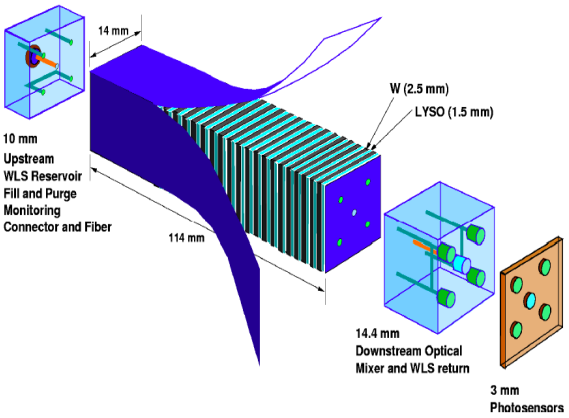

Figure 7: The EE Shashlik configuration based upon interleaved W and LYSO layers. Twenty-nine LYSO crystals and twenty-eight W plates comprise the module. Four WLS quartz capillaries are used to read out the scintillation light from the tiles. A central calibration fiber is used for monitoring. (An alternative technology uses the same sampling structure and thicknesses, but has CeF_3 replacing the LYSO.)

Two different options for the light extraction have been proposed: the *shashlik* configuration (Fig. 7) with the wave-length shifting (WLS) quartz capillaries running inside the crystals and a more standard configuration with the fibers located along the depolished chamfers of the channel.

Beam tests of Shashlik detectors have been performed at Fermilab. A supermodule containing 16 shashlik modules in a 4x4 array has been tested with muon, electron and pion beams with energy up to 120 GeV at the MTest facility at Fermilab. Analysis of the data is currently underway. Beam tests of a W/CeF_3 module read out with WLS fibers in a beam of 491.4 MeV electrons at Frascati have also been completed few months ago. Figure 8 shows the energy

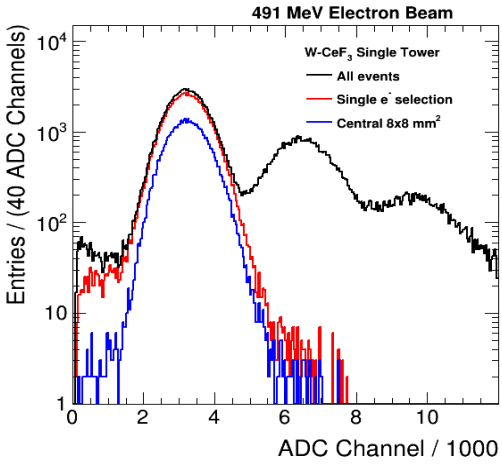

Figure 8: Energy spectrum of the W/CeF_3 channel tested with 491 MeV electron beam in Frascati. Single, double and triple electron peaks are clearly visible (black distribution). Spectra obtained with single electron selection criteria are also shown.

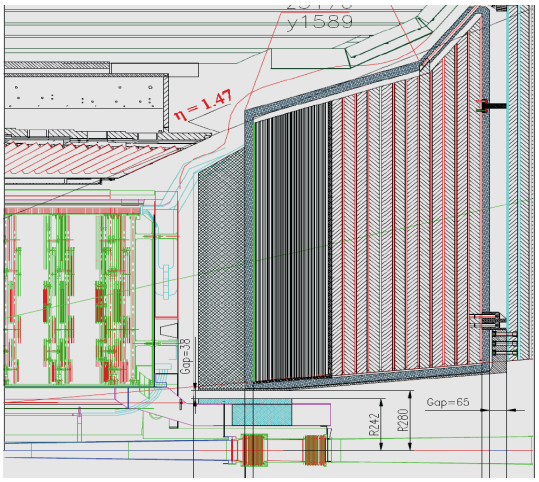

Figure 9: Sketch of a possible structure of HGC. The E-HG has its front face at the same location as the front face of the current EE. Directly behind it there is the H-HG, which is a 3.5 λ silicon-brass calorimeter. Behind that is a 5.5 λ backing hadron calorimeter, which, since the radiation levels are low, could use the same technology as the current HE.

spectrum of the CeF_3 where multiple electrons interacting in the structure can be clearly resolved and spectra obtained with single electron selection using external beam line devices are also shown [11]. Further data analysis is ongoing. Both configuration will be tested soon at CERN in H4 area.

5.2. *High Granularity Endcap Calorimeter*

A dense high-granularity calorimeter running in the High Luminosity LHC offers the opportunity of high performance in the presence of high pile-up environment of the forward (endcap) regions providing very high resolving power for single particles and jets and a good jet energy resolution also exploiting the particle flow technique.

The overall design of the high-granularity calorimeter, HGC, is shown in Fig. 9. Moving outwards from the interaction region, the volume begins near the location of the front face of the current electromagnetic endcap calorimeter with a tungsten/lead-silicon sampling electromagnetic calorimeter, the E-HG, with a depth of 25 X_0 and about 1 λ. This is followed by a brass-silicon hadron calorimeter, 3.5 λ deep, the H-HG, which is followed by a 5.5 λ brass-scintillator sampling backing calorimeter, the B-HG, to bring the total calorimeter depth to 10 λ.

The E-HG and H-HG will use planes of silicon as the active medium, while the B-HG, situated where the radiation levels are low, can be constructed with either plastic scintillator, as is the current HE, or with GEM or Micromegas gas chambers.

In this structure there will be only a small gap between the electromagnetic and hadron calorimeters, which is expected to improve the jet energy measurements. Additionally, by bringing the hadron calorimeter into the space currently used for the EE electronics, there will be space behind the B-HG where the radiation levels will be sufficiently low so that not only electronics stations and other services, but also additional muon chambers could be situated.

For E-HG a variable longitudinal sampling is proposed, determined by the absorber thickness:

- 10 layers: 0.5 X_0 thickness absorber followed by a plane of silicon,
- 10 layers: 0.8 X_0 thickness absorber followed by a plane of silicon,
- 10 layers: 1.2 X_0 thickness absorber followed by a plane of silicon.

Most of the calorimeter uses cells of 0.9 cm^2. There will be six million cells in the E-HG for a surface of 420 m^2 of silicon. The absorber layers are composed of tungsten in an alveolar mechanical structure, and copper/lead in the units which slide into the alveolar structure. A similar configuration, but with tungsten as the absorbing material, has been studied in test beams by the CALICE collaboration for future ILC/CLIC detectors and, when instrumented with 525 micron-thick silicon sensors, gave an energy resolution of around $16.5\%/\sqrt{E}$ with a linear energy response [12].

6. Pile-Up mitigation with precise timing

Although precise time measurement has not been a primary goal of calorimeters at hadron colliders, during LHC Run1 the CMS ECAL measured the timing of electrons from Z decays with an excellent resolution, about 200 ps [13]. During HL-LHC a more precise timing may allow the subtraction of spurious energy deposits coming from pile-up, help identify pile-up jets, and improve the estimation of the position of the production vertex for di-photon events.

A time measurement with precision of a few tenths of ps would allow the association of energy deposits to the primary vertex from which they originate within 1 cm, thus reducing significantly the probability of misreconstructing photons and electrons. R&D is ongoing to determine if such a goal can be obtained by adding a dedicated timing detector or by introducing more sophisticated timing capabilities to the new electronics in EB and to the new EE detector. For a dedicated detector, micro-channel plates for direct ionization measurement, gas electron multipliers, and avalanche photodiode detectors are being investigated. If a pre-radiator were included, such detectors could provide timing information for both neutral and charged particles.

The current ECAL geometry has been used in a simplified study using Geant where crystals are divided in different longitudinal sub-cells. In each sub-cell the timing information is extracted by averaging the time of simulated hits within that volume, weighted by the energy of each deposit, restricting to deposits of energy above 5 keV. The optimal thickness and position of the subcell has been studied in terms of intrinsic spread of the timing information. The smallest spread is obtained for 1 cm thick layer when there are about 8-10 radiation lengths in front of it, i.e. at the maximum of the shower. The time spread as a function of depth for photons of transverse momentum of 25 GeV is shown in the Figure 10 and is less than 10 ps already after 2 X_0.

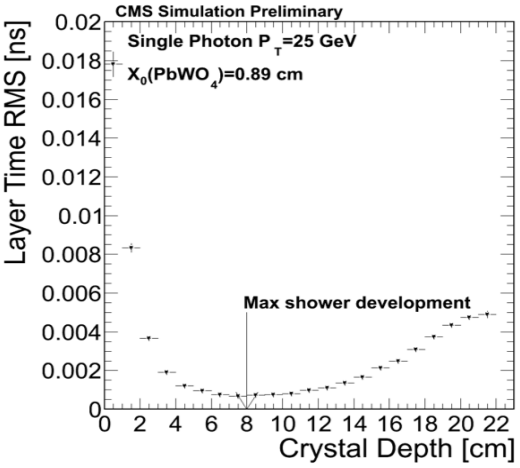

Figure 10: Intrinsic spread of the Geant hits time for 25 GeV p_T photons as a function of the crystal depth with 1 cm thick layers.

7. Conclusions

The High Luminosity LHC environment poses severe requirements to detectors in terms of performance and radiation hardness. We have shown that the ECAL barrel will survive up to 3000 fb^{-1} providing good performance during HL-LHC while the ECAL endcaps should be replaced at the end of the LHC Phase 1 (after 500 fb^{-1}). Two new endcap calorimeter options are being studied: a sampling calorimeter composed of tungsten absorber and LYSO or CeF3 scintillators and a high granularity calorimeter (HGC). Finally we discussed the possibility to provide precise timing resolution, which may add important information for pile-up mitigation.

References

[1] CMS Collaboration, "The CMS experiment at the CERN LHC", *JINST* **3** (2008) S08004
[2] P. Adzic *et al.*, "Radiation hardness qualification of PbWO4 scintillation crystals for the CMS Electromagnetic Calorimeter", *JINST* **5** (2010) P03010
[3] M. Huhtinen *et al.*, "High-energy proton induced damage in PbWO4 calorimeter crystals", *Nucl. Instrum. Meth.* **A545** (2005), 63-87
[4] E. Auffray *et al.*, "Experimental study of the lead tungstate scintillator proton-induced damage and recovery", *IEEE Trans. Nucl. Sci.* **59 n.5** (2012) 2219-2223
[5] M.T. Lucchini *et al.*, "Test beam evaluation of CMS ECAL Endcap Supercrystals constructed from hadron-damaged crystals", CMS DN-2013/007
[6] I. Azhgirey and V.Talanov, "Proc. of XVIII Workshop on the Charged Particles Accelerators", Technical Report CMS-2005-010, (2000)
[7] GEANT4 Collaboration, "GEANT4 - a simulation toolkit", *Nucl. Instrum. Meth.* **A506** (2003) 250
[8] F. Gentit, "Litrani: A General purpose Monte Carlo program simulating light propagation in isotropic or anisotropic media", *Nucl.Instrum.Meth.* **A486** (2002) 35-39
[9] S. Baccaro *et al.*, "Radiation damage effect on avalanche photodiodes", *Nucl.Instrum.Meth.* **A426** (1999) 206-211
[10] G. Battistoni, F. Cerutti, A. Fasso' *et al.*, "The FLUKA code: Description and benchmarking", *AIP Conf. Proc.* **896** (2007)
[11] P. Meridiani *et al.*, to be published in Proc. IEEE NSS 2014
[12] C. Adloff, Y. Karyotakis, J. Repond *et al.*, "Response of the CALICE Si-W electromagnetic calorimeter physics prototype to electrons", *Nucl.Instrum.Meth.* **A608** (2009) 372-383
[13] CMS Collaboration, "Energy calibration and resolution of the CMS electromagnetic calorimeter in pp collisions at sqrt(s) = 7 TeV", *JINST* **8** (2013) P09009